ISSN 1027-4510, Journal of Surface Investigation: X-ray, Synchrotron and Neutron Techniques, 2018, Vol. 12, No. 6, pp. 1182–1189. © Pleiades Publishing, Ltd., 2018.

Determination of the Thickness of Nanofilms Using X-Ray Photoelectron Spectroscopy

P. S. Kaplya[a], D. S. Efremenko[b], and V. P. Afanas'ev[a, *]

[a] *National Research University "Moscow Power Engineering Institute", Moscow, 111250 Russia*

[b] *Deutsches Zentrum für Luft- und Raumfahrt (DLR), Institut für Methodik der Fernerkundung (IMF), Oberpfaffenhofen, 82234 Germany*

**e-mail: v.af@mail.ru*

Received January 25, 2018

Abstract—Determination of coating thicknesses whose dimensions lie in the nanometer range is an important analytical application of X-ray photoelectron spectroscopy (XPS). The coating thickness is determined as a result of comparing peak intensities measured using lines corresponding to the coating with those of characteristic substrate lines. It is shown that the error in determining thicknesses using a procedure that completely disregards processes of elastic electron scattering reaches 50%. At present, the influence of elastic scattering processes is taken into account by replacing the inelastic mean free path with the fitting parameter called the effective attenuation length. Physical phenomena occurring in the case of the inclusion of an elastic photoelectron scattering channel are analyzed in this paper. Two approaches to the description of XPS spectra are considered: the first one is implemented using invariant embedding methods, and the second one used the method of discrete ordinates with the matrix exponent. On the basis of the first method, the influence of multiple elastic-scattering events on the XPS energy spectra is studied. The second one shows a high effectiveness when calculating no loss peaks of photoelectrons emitted by multilayer samples.

Keywords: electron spectroscopy, X-ray photoelectron spectroscopy (XPS), elastic electron scattering, transfer equation, invariant embedding, effective attenuation length

DOI: 10.1134/S1027451018050580

INTRODUCTION

In 1974, Fadley and his colleagues [1] showed the possibility of determining the layer thickness of material deposited onto a substrate made of another material. To do this, it was necessary to find the ratio of intensities of no loss peaks of the coating and the substrate (1). Theoretical description [1] was based on an approximation completely ignoring elastic-scattering processes: the concept of the photoemission process, in which photoelectrons move in a medium along straight lines, experiencing only inelastic collisions. This approximation is called the straight-line approximation (SLA) and underlies modern XPS theories [2, 3]. Because the elastic-scattering cross section σ_{el} is on the same order as the inelastic scattering cross section σ_{in} and is even slightly larger than the inelastic one in cases that are characteristic for XPS experiments (Fig. 1), disregarding the processes of elastic photoelectron scattering can lead to significant errors in the interpretation of XPS signals.

In this paper, we limit ourselves to considering two-layer targets consisting of a substrate and a layer of material that differs from that of the substrate. Considering two-layer targets, we remember that the surface layer (and sometimes layers), in which the energy loss cross section $\omega_{in S}(\Delta)$ differs from the cross section $\omega_{in B}(\Delta)$, which is valid for the homogeneous bulk located at a distance from the surface, exists even in a homogeneous target. Therefore, it is more adequate to speak about a target made of two materials, but the number of layers in the target can be much larger than two 2.

Because the mean free path of an X-ray quantum exceeds that of an electron between successive inelastic collisions by several orders: $l_{in} = 1/n\sigma_{in}$, where n is the concentration of target atoms, we assume that the distribution of photoelectron sources in the target is uniform. Using the SLA approximation [1–3], we obtain:

$$Q_2(z_2)/Q_1(\infty) = \frac{Q_2(\infty,\mu,\mu_0,\varphi)}{Q_1(\infty,\mu,\mu_0,\varphi)}\frac{\left[1-\exp\left(-\frac{z_2}{l_{in2}\mu}\right)\right]}{\exp\left(-\frac{z_2}{l_{in2}\mu}\right)}. \quad (1)$$

The density of the photoelectron flux emitted by a semi-infinite homogeneous layer determines the following expression:

$$Q_k(\infty,\mu,\mu_0,\varphi) = I_{ink}\mu F_k(\mu,\mu_0,\varphi), \quad (2)$$

which contains the quantities known in [4–7]: I_{ink} is the mean free path between inelastic collisions [7, 8], $F_k(\mu,\mu_0,\varphi)$ is the differential photoionization cross section [4, 5], and μ is the cosine of the photoelectron departure angle to the normal. Thus, in formula (1), the unknown quantity is only the coating thickness z_2:

$$z_2 = I_{in2}\mu \ln\left[\frac{I_{in1}F_1(\mu,\mu_0,\varphi)}{I_{in2}F_2(\mu,\mu_0,\varphi)}\frac{Q_2}{Q_1} + 1\right]. \quad (3)$$

The currently existing procedure taking elastic scattering processes into account [2, 3] was developed in the 1990s and is noticeably dated. The problems of multiple particle scattering in multilayer structures that are analogous to ones considered in this paper appear when identifying signals of remote probing of the atmosphere [8–14]. The methods developed in [8–14] give a consistent solution, which precisely takes into account all factors of the albedo elastic scattering of particles moving in layered inhomogeneous targets.

When determining the layer thickness, we encounter an ill-defined problem having many solutions. The fitting procedure is the most reliable method for solving such problems. To conveniently implement the indicated problem, it is necessary to have a high-speed calculation procedure. It is obvious that Monte Carlo (MC) simulation is not adequate in this case. The small-angle approximation having a high operation speed does not always make it possible to carry out the calculation with satisfactory error; in the case of targets with high atomic numbers, the error reaches 10%. The error of the transport approximation is inadmissibly high; it gives qualitatively incorrect results in the description of electron propagation through material layers whose thicknesses are smaller than the transport path.

In this paper, (i) we construct a mathematical model that consistently takes into account processes of multiple elastic and inelastic scattering events, it is equivalent to the real process of the photoemission of a layered inhomogeneous sample and (ii) methods of optical scattering theory are adapted to electron-scattering problems and are used to find analytical and efficient numerical solutions to problem of determining multilayer coating thicknesses. We emphasize that, to solve the inverse problems considered in this paper by means of the fitting method, the operation speed is crucial.

Figure 2 shows that the SLA error reaches 50% for the most important probing angles of an electron beam. The error behaves nonmonotonically as the viewing angle varies. Calculations show that the error is a function of the upper-layer thickness. The indicated factors show that it is impossible to describe the experimental results by replacing I_{in2} in (1) with a fitting length called the effective attenuation length (EAL) [2, 3]. Calculations using the technique in [12–14] for a target consisting of tens of layers are carried out in fractions of a second. The modern procedure [2, 3] does not exceed the limits of two-layer samples.

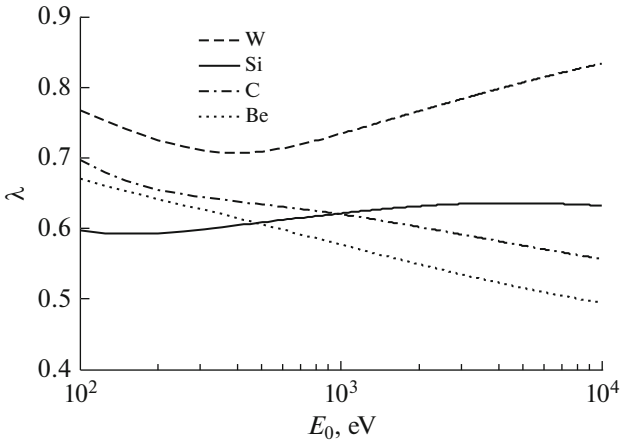

Fig. 1. Albedo for single scattering $\lambda = \sigma_{el}/(\sigma_{el} + \sigma_{in})$.

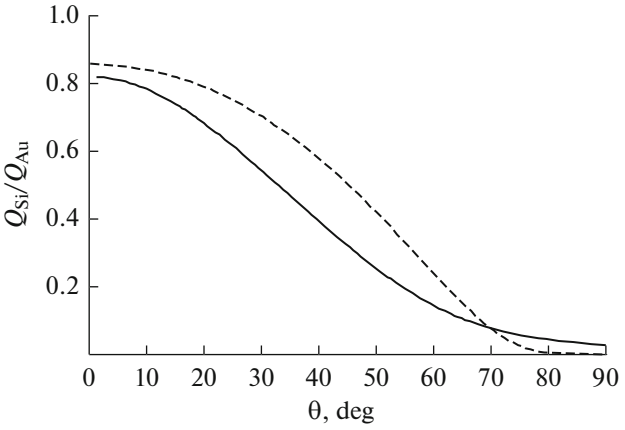

Fig. 2. Dependence of the ratio of the Au 4*f*5/2 peak intensity to the Si 2*s* peak intensity for a 2.5-nm Si/Au target on the viewing angle. Probing is along the normal: the SLA is denoted by the dashed line; and exact calculation in accordance with [12–14], by the solid line.

THEORETICAL INTRODUCTION

The aim of this paper is to construct a model that consistently describes photoemission processes when probing a surface by means of X-ray radiation and analyze the physical principles of processes occurring

when the elastic channel of photoelectron scattering is taken into account.

The consistent procedure of the description of the XPS process leads us to the equation for the photoelectron flux density $Q(\tau, p, \mu_0, \mu, \varphi)$ [15]:

$$\frac{\partial}{\partial\tau}Q_k(\tau,\mu_0,\mu,\varphi)+\frac{1}{\mu}Q_k(\tau,\mu_0,\mu,\varphi)$$
$$-\frac{(1-\lambda)}{\mu}Q_{k-1}(\tau,\mu_0,\mu,\varphi)$$
$$=\delta_{k0}\lambda_\gamma f(\mu_0,\mu,\varphi)+\lambda_\gamma\int_0^{2\pi}\int_{-1}^{0}f(\mu_0,\mu',\varphi'-\varphi)$$
$$\times R_k(\tau,\mu',\mu,\varphi')\frac{d\mu'}{\mu'}d\varphi' \qquad (1)$$
$$+\lambda\int_0^{2\pi}\int_0^{1}Q_k(\tau,\mu_0,\mu',\varphi'-\varphi)\,x_{\rm el}(\mu',\mu,\varphi')\frac{d\mu'}{\mu'}d\varphi'$$
$$+\lambda\sum_{m=0}^{k-1}\int_0^{2\pi}\int_0^{2\pi}\int_0^{1}\int_0^{1}Q_{k-m}(\tau,\mu_0,\mu',\varphi')\int_{-1}^{0}x_{\rm el}\left(\mu',\mu'',\varphi''-\varphi'\right)$$
$$\times R_m\left(\tau,\mu'',\mu,\varphi''-\varphi\right)\frac{d\mu'}{\mu'}d\varphi'\frac{d\mu''}{\mu''}d\varphi'',$$

where

$$f(\mu,\mu_0,\varphi)=\frac{1}{4\pi}\sum_{i=0}^{3}B_iP_i(\psi),\quad B_0=1,$$
$$\cos\psi=\mu\mu_0-\sqrt{\left(1-\mu^2\right)\left(1-\mu_0^2\right)}\cos\varphi$$

is the angular distribution of the photoionization cross section [7, 8]; R is the function of the reflected electron flux density (the reflection function) [16, 17]; $\sigma_{\rm el}$ and $\omega_{\rm el}$ are the total and differential cross sections for single electron scattering; $x_{\rm el}(\mu',\mu'',\varphi''-\varphi')$ is the differential cross section for elastic electron scattering normalized to unity; and $\sigma_{\gamma\to e}$ is the photoionization cross section, $\lambda_\gamma=\sigma_{\gamma\to e}/(\sigma_{\rm el}+\sigma_{\rm in})$.

The boundary condition for Eq. (1) is given by

$$Q(0,p,\mu_0,\mu,\varphi)=0. \qquad (2)$$

In accordance with the concept of partial intensities [15], the subscript k of the function $Q_k(\tau,\mu_0,\mu,\varphi)$:

$$Q(\Delta,\mu_0,\mu,\varphi)$$
$$=Q_0(\tau,\mu_0,\mu,\varphi)\delta(\Delta)+\sum_{k=1}^{\infty}Q_k(\tau,\mu_0,\mu,\varphi)\,x_{\rm in}^k(\Delta), \qquad (3)$$

determines the contribution to the energy spectrum of the X-ray photoelectron emission of processes of k-fold inelastic scattering. Equation (1) gives the possibility of tracing the influence of the elastic scattering process on XPS spectrum formation: SLA is the solution of Eq. (1); however, all terms except the first one on the right-hand side are omitted in it. We let the index NS (numerical solution) denote the asymptotically exact numerical solution of Eq. (1), in which all terms on the right-hand side are taken into account.

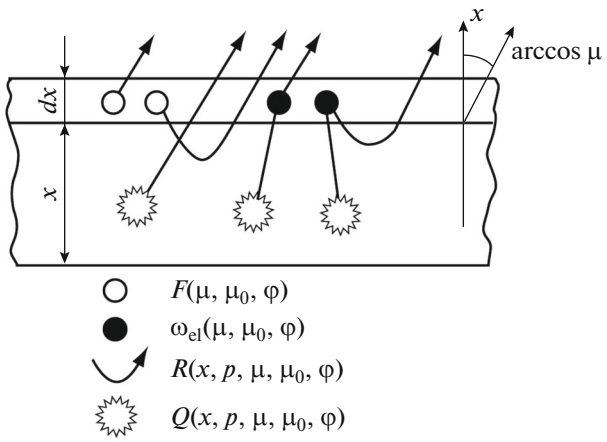

Fig. 3. Processes leading to a change in the photoemission flux density in the case where a thin ($n\sigma dx \ll 1$) film of the same material was added above.

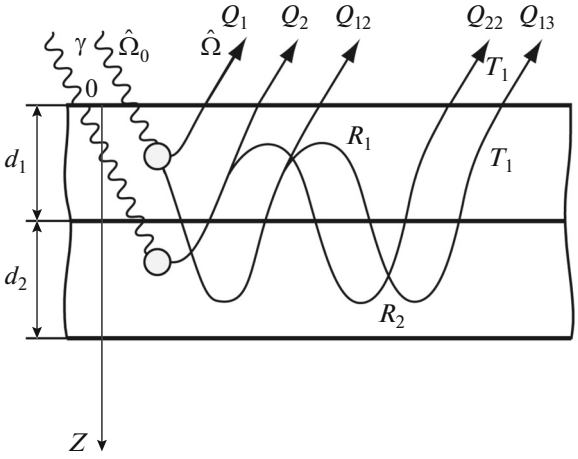

Fig. 4. Processes of only elastic scattering of photoelectrons generated in the upper layer (1) and the substrate (2) before the output to free space at the recording angle.

Equation (1) is written on the basis of analysis of the processes shown in Fig. 3. Solving Eq. (1), we can study the physical principles of assumptions to which disregarding any given term in (1) leads.

CALCULATION OF THE DENSITY OF THE PHOTOELECTRON FLUX EMITTED BY LAYERED INHOMOGENEOUS TARGETS

The problems of electron scattering at multilayer systems are of greatest interest for applications. We

describe the formation process of the energy spectrum of XPS emission by a two-layer system in accordance with the scheme shown in Fig. 4.

In accordance with Fig. 4, the flux density function of electron photoemission by a two-layer system can be described by the following formula:

$$\begin{aligned} Q &= Q_1 + Q_{12} + Q_{13} + \ldots + Q_2 + Q_{22} + Q_{23} + \ldots \\ &= Q_1 + (Q_2 + Q_1 \otimes R_2) \otimes (\delta + R_1 \otimes R_2 + R_1 \otimes R_2 \otimes R_1 \otimes R_2 + \ldots) \otimes (\mu L_1 + T_1), \end{aligned} \quad (4)$$

where Q_i, R_i, and T_i are the function of the photoelectron flux density and the functions of the reflection and transmission of a layer of the i-th material, respectively; L_i is the Landau function (5); and the operator $\otimes$ is defined by the triple integral (6):

$$L(s,\Delta) = e^{-(1-\lambda)\frac{s}{l_{\text{tot}}}} \sum_{k=0}^{\infty} \left[(1-\lambda)\, x_{\text{in}}^{k}(\Delta) \frac{s}{l_{\text{tot}}} \right]^k \frac{1}{k!}, \quad (5)$$

$$\begin{aligned} Q_2 \otimes T_1 = \int_0^{\Delta} \int_0^{2\pi} \int_0^{1} & Q(\tau_2, \varepsilon, \mu_0, \mu', \varphi') \\ & \times T(\tau_1, \Delta - \varepsilon, \mu', \mu, \varphi - \varphi') \frac{d\mu'}{\mu'} d\varphi' d\varepsilon. \end{aligned} \quad (6)$$

The notation in [15–16] is used in expressions (4)–(6). We use the obtained formulas to analyze the effects to which leads the inclusion of multiple elastic scattering in the process of the formation of XPS spectra of two-layer samples.

The calculations shown in Fig. 3 were obtained using formula (3), in which the coefficients $Q_k(\tau, \mu_0, \mu, \varphi)$ are the result of the exact numerical solution of Eq. (1); the differential inelastic scattering cross sections $x_{\text{in}}(\Delta)$ were determined in accordance with the Werner paper [18]; the dashed line corresponds to $Q_{\text{Si}}(\tau, \mu_0, \mu, \varphi)$ (the photoemission spectrum of a free Si layer); and the solid curve was obtained as a result of the calculation using formula (4) (the photoemission spectrum of a Si layer deposited on a Au substrate). It follows from the results shown in Fig. 5 that the influence of the underlying surface on the no loss peak formed by photoelectrons of the Si $2s_{1/2}$ line, which were beyond the inelastic-scattering channel, is extremely insignificant. But the Au substrate led to a four-fold increase in the photoemission signal in the range where the energy losses are about 100 eV.

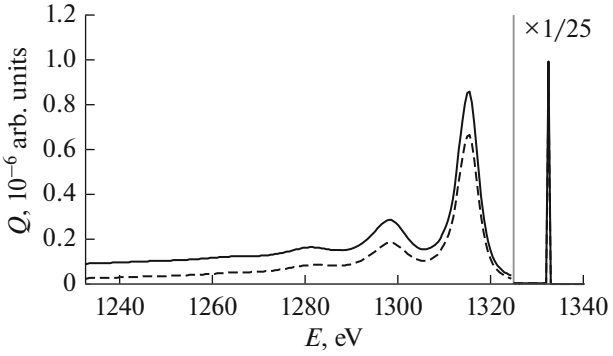

Fig. 5. Energy spectrum of photoelectrons emitted by a 2.5-nm Si layer deposited onto a semi-infinite Au substrate at the $2s_{1/2}$ line. The no loss peak is isolated on the right and is presented on a scale that differs from the region (presented in the left part) of photoelectrons losing their energy during the inelastic-scattering process. Probing is along the normal, and the polar viewing angle is 20°. The solid line corresponds to the calculation taking into account the processes of photoelectron reflection from the Au substrate; and the dashed line, to that without the inclusion of these processes.

We analyzed the influence of the processes of multiple elastic scattering on the intensity of coating photoemission (material—2) and that on the emission of the underlying layer. We consider the influence of multiple scattering processes in the coating on the intensity of the underlying-layer photoemission. Papers studying the effect of the "rotation of the brightness body" were dedicated to detailed discussion of the variation in the characteristics of electron fluxes propagating through material layers [19]. Figure 6 shows the energy spectra near the Si $2s_{1/2}$ line. We studied the influence of a Au coating on the intensity of Si photoemission. It can be seen that the influence is maximum in the no-loss peak range and decreases as the energy losses of Si $2s_{1/2}$ photoelectrons increase. The results shown in Figs. 5 and 6 demonstrate that elastic-scattering processes drastically affect the XPS signal background.

In the Tougaard paper [20], it was shown that the same peak intensity is observed for different distributions of the analyzed material in the sample under study. But in the case of the same areas under the no loss peaks, the energy loss spectra are very different (the ranges in the left parts of Figs. 5 and 6). However, in [20], the calculations were carried out without considering elastic-scattering processes, Figs. 5 and 6 illustrate strikingly the scale of errors appearing in this case; therefore, the results in [20] must be considered as qualitative. Tougaard [20] stated once more that determination of the coating thickness is an inverse

problem that is ill-defined from the mathematical point of view. To obtain unambiguous results on the coating profile, it is necessary to implement one of three procedures: (i) to perform measurements in different geometries; (ii) to perform energy scanning, carrying out measurements using different X-ray sources (for example, using Al and Mg cathodes); and (iii) to analyze the energy loss spectrum on the basis of consistent methods taking elastic- and inelastic-scattering channels into account.

DESCRIPTION OF SCATTERING PROCESSES IN MULTILAYER STRUCTURES BASED ON THE METHOD OF DISCRETE ORDINATES WITH THE MATRIX EXPONENT

The process of XPS signal formation in multilayer systems can be described within the framework of the theory developed above and based on solution of the boundary-value problem by means of the invariant embedding method. But it follows from Fig. 4 and formula (4) that, within the framework of the developed approach, it is necessary to sum infinite series. In the developed approach, we restrict ourselves to the first two terms, understanding that the contribution from the next term is less than the obtained result by two orders, without analyzing the problem of the error appearing when summing the infinite series. Below we present an approach that is capable of summing the infinite series (4). We present a procedure for solution of the boundary-value problem based on the method of discrete ordinates with the matrix exponent, but it is applicable only to the solution of albedo problems, i.e., problems that are unable to describe energy spectra, but can calculate the XPS no-loss peak intensities.

Consideration of the transport of only elastically scattered electrons leads us to the equation obtained when considering the problem of radiation transfer in turbid media in the case of sources uniformly distributed in the medium. The equation has the form:

$$\mu\frac{\partial Q_0(\tau,\mu,\varphi)}{\partial\tau} = -Q_0(\tau,\mu,\varphi) - \frac{\lambda}{4\pi}\int_0^{2\pi}\int_{-1}^{1} Q_0(\tau,\mu,\varphi-\varphi')\,x_{\rm el}(\mu',\mu,\varphi')\,d\mu' d\varphi' + \lambda_\gamma f(\mu,\mu_0,\varphi). \quad (7)$$

The last term describes the distribution of internal sources in the medium. We seek the functions Q_0, $x_{\rm el}$, and f in the form of coefficients of the expansion in a Fourier series:

$$Q_0(\tau,\mu,\varphi) = \sum_{m=0}^{2M-1}(2-\delta_{m0})\,Q_{m0}(\tau,\mu)\cos(m\varphi),$$

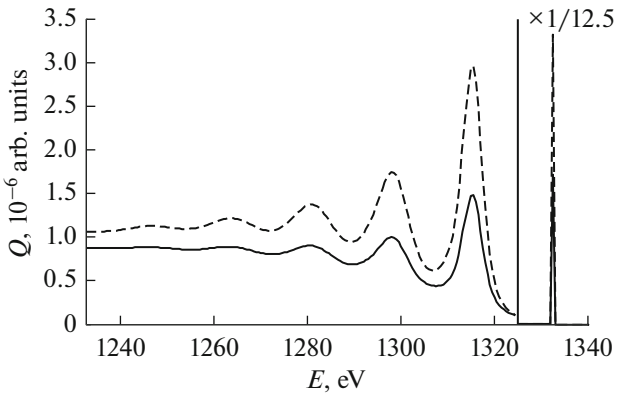

Fig. 6. Intensity of Si photoemission: the dashed line corresponds to the pure semi-infinite Si bulk; and the solid curve, to the Si bulk coated with a 1-nm Au layer.

$$x_{\rm el}(\tau,\mu,\varphi) = \sum_{m=0}^{2M-1}(2-\delta_{m0})\,x_{\rm mel}(\tau,\mu)\cos(m\varphi),$$

$$f(\tau,\mu,\varphi) = \sum_{m=0}^{2M-1}(2-\delta_{m0})\,f_m(\tau,\mu)\cos(m\varphi).$$

Their substitution into Eq. (7) makes it possible to exclude the dependence on the azimuthal angle (for convenience, we omit the subscript m):

$$\mu\frac{\partial Q_0(\tau,\mu)}{\partial\tau} = -Q_0(\tau,\mu,\varphi) - \frac{\lambda}{2}\int_{-1}^{1} Q_0(\tau,\mu)\,x_{\rm el}(\mu',\mu)\,d\mu' + \lambda_\gamma f(\mu,\mu_0). \quad (8)$$

The majority of numerical methods for solving Eq. (7) were obtained when considering optical problems. The method of discrete ordinates [10] and the addition–doubling method [11] were based on replacement of the integral in Eq. (8) with the Gauss–Legendre quadrature $\{\mu_k, w_k\}_{k=1,\ldots,2N}$, where μ_k and w_k are discrete ordinates and the quadrature balance, respectively. In this case, N discrete ordinates ($\mu_k > 0$) belong to the upper hemisphere; and the same number of ordinates ($\mu_k < 0$), to the lower one. The continuous dependence of functions Q is replaced with the discrete one:

$$\mathbf{q}^{\pm}(\tau) = [Q(\tau,\pm\mu_k)], \quad k = 1,\ldots,N.$$

Using the described discretization procedure, for each layer, we obtain a system of differential equations:

$$\frac{d\mathbf{q}(\tau)}{d\tau} = -\mathbf{A}\mathbf{q}(\tau) + \mathbf{f}, \quad (9)$$

where the layer matrix $\mathbf{A}$ has the block–diagonal form:

$$\mathbf{A} = \begin{bmatrix} \mathbf{A}_{11} & \mathbf{A}_{12} \\ -\mathbf{A}_{12} & -\mathbf{A}_{11} \end{bmatrix},$$

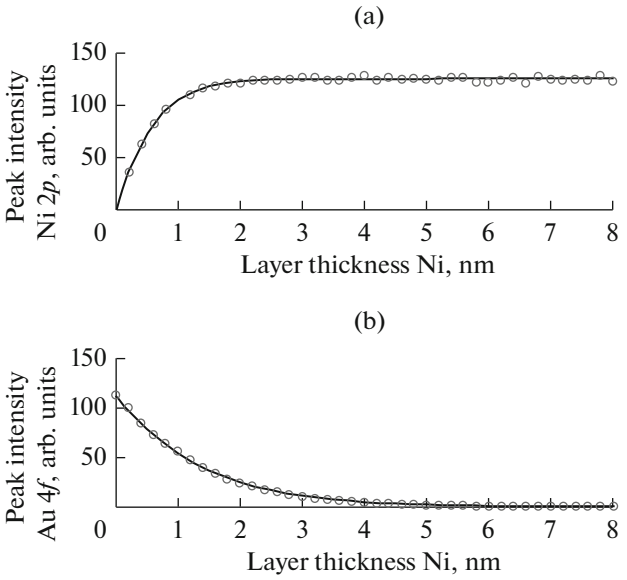

Fig. 7. Dynamics of the change in the radiation intensity of (a) the Ni layer at the 3*p* line and (b) Au layer at the 4*f* line as the thickness of the coating Ni layer increases. The solid line corresponds to the results of numerical calculation based on the procedure given in this paper. The open circles correspond to MC simulation [21].

and

$$\mathbf{A}_{11} = \mathbf{M}\mathbf{S}^{+}\mathbf{W} - \mathbf{M}, \quad \mathbf{A}_{12} = \mathbf{M}\mathbf{S}^{-}\mathbf{W}, \quad \mathbf{f} = \begin{bmatrix} \mathbf{M}\mathbf{f}^{+} \\ -\mathbf{M}\mathbf{f}^{-} \end{bmatrix}, \quad \mathbf{f}^{\pm} = \lambda_{\gamma} f\left(\mu^{\pm}\right),$$

$$\left[\mathbf{S}^{\pm}\right]_{kl} = \frac{1}{2}\omega x\left(\mu_k^{\pm}, \mu_l\right), \quad [\mathbf{W}]_{kl} = w_k \delta_{kl}, \quad [\mathbf{M}]_{kl} = \frac{\delta_{kl}}{\mu_k}.$$

The solution of system (9) by means of the matrix exponent method was obtained in [12]. Namely, we integrate Eq. (9):

$$\mathbf{q}(\tau) = e^{-\mathbf{A}\tau}\mathbf{q}(0) - \int_0^{\tau} e^{\mathbf{A}(\tau'-\tau)}\mathbf{f}d\tau'. \qquad (10)$$

Then, considering spectral decomposition of the layer matrix

$$e^{-\mathbf{A}\tau} = \mathbf{U}e^{-\mathbf{\Lambda}\tau}\mathbf{U}^{-1},$$

where $\mathbf{U}$ is the matrix of eigenvectors and $\mathbf{\Lambda}$ is the diagonal matrix of eigenvalues, we obtain Eq. (10) in the form

$$\mathbf{q}(\tau) = \mathbf{U}e^{-\mathbf{\Lambda}\tau}\mathbf{U}^{-1}\mathbf{q}(0) - \int_0^{\tau} \mathbf{U}e^{\mathbf{\Lambda}(\tau'-\tau)}\mathbf{U}^{-1}\mathbf{f}d\tau'.$$

After integration, we obtain

$$\mathbf{q}(\tau) = \mathbf{U}e^{-\mathbf{\Lambda}\tau}\mathbf{U}^{-1}\mathbf{q}(0) - \mathbf{U}\left(\frac{e^{\mathbf{\Lambda}\tau}}{\mathbf{\Lambda}} - 1\right)e^{-\mathbf{\Lambda}\tau}\mathbf{U}^{-1}\mathbf{f}. \qquad (11)$$

Equation (11) is obtained for each of the layers. All equations are collected to form the system, which is supplemented with the boundary conditions: $\mathbf{q}^{-}(0) = 0$, $\mathbf{q}^{+}(\tau_{\text{bottom}}) = 0$, where τ_{bottom} is the thickness of the entire target.

Numerical aspects of the described procedure were considered in [13, 14].

The results of MC simulation in [21] are compared with those of the above numerical calculation in Fig. 7. Almost instantaneous numerical calculation gives results with an error that is noticeably smaller than the MC simulation data.

Based on the results indicated in Fig. 7 and similar, but obtained for peaks corresponding to other transitions, we obtain the dependences of the relative intensities on the coating thickness. These dependences are given in the right part of Fig. 8. Comparing the experimental and calculated data: drawing horizontal lines from the left graph in Fig. 8 to the right one, we obtain the sought thicknesses. The Ni-layer thicknesses determined using the proposed method correspond to quantities presented in [21] for all given combinations of lines. Figure 9 shows the methodological error, which appears as a result of neglecting processes of reflection from the Au substrate.

CONCLUSIONS

In this paper, we have noted the physical effects associated with the processes of elastic photoelectron scattering, which lead to a change in the intensities of no loss peaks and radically affect the process of the measurement of layer dimensions by means of XPS methods. Efforts to describe the XPS signal formation process in the SLA approximation, but with subsequent replacement of the mean free inelastic path with the fitting parameter called the "effective attenuation length" (EAL) were associated with a series of problems. The quantity EAL depends on the layer thickness, from which follows the necessity of the self-consistency procedure in the process of calculation of the layer thickness. The EAL quantity also depends on the scattering angle, the layer material and, as shown in this work, on the substrate material. Because the inverse problem, which is ill-defined from the mathematical point of view, was solved, the operation with one fitting parameter in the SLA can lead to significant uncontrolled errors and methodological errors.

The practice of operation with the method of discrete ordinates with the matrix exponent used in this paper and based on the ideas and procedures presented in [8–14] indicates the high efficiency of determination of the coating thicknesses: the dependence of the coating thickness on the ratio of the intensities was calculated (Fig. 8), using which and having the experimental data, we obtained the coating thick-

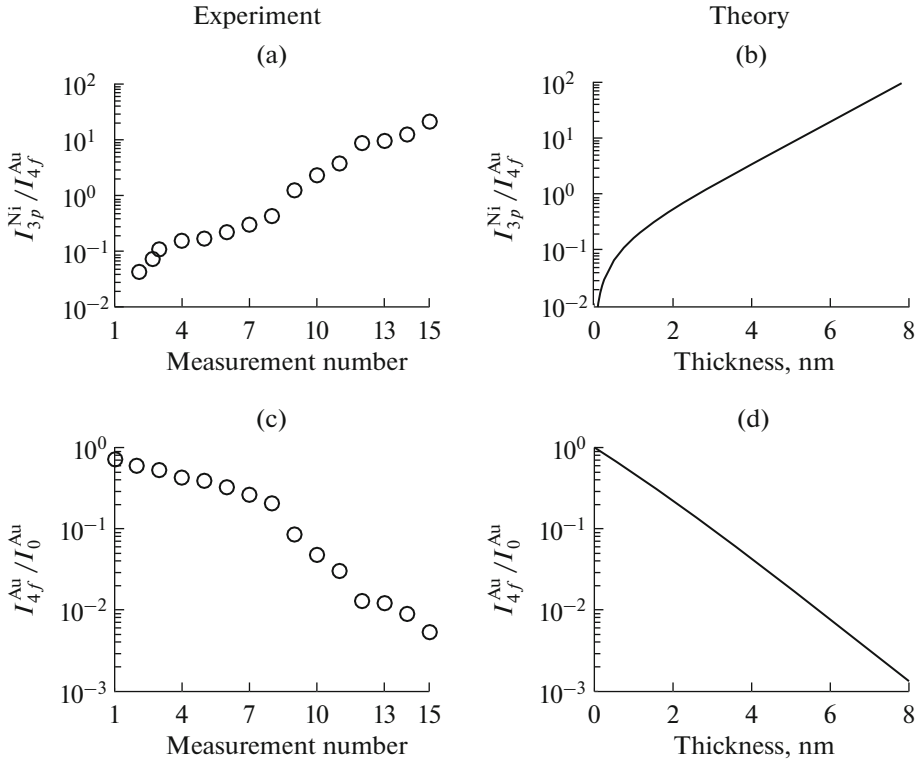

Fig. 8. Ratios of the peak intensities (b) $I_{3p}^{Ni}(d_{Ni})/I_{4f}^{Au}(d_{Ni})$ and (d) $I_{4f}^{Au}(d_{Ni})/I_{4f}^{Au}(0)$ calculated on the basis of the presented procedure as functions of the Ni-layer thickness d_{Ni}. The experimentally measured ratios of the intensities (a) $I_{3p}^{Ni}(d_{Ni})/I_{4f}^{Au}(d_{Ni})$ and (c) $I_{4f}^{Au}(d_{Ni})/I_{4f}^{Au}(0)$ [21].

nesses. To carry out the method of discrete ordinates with the matrix exponent, it is necessary to have: (i) the values of the mean inelastic path lengths for the substrate and coating components (the TPP-2M formula [22, 23] was used in this paper) and (ii) differential elastic-scattering cross sections (the data in [23] were used in this paper).

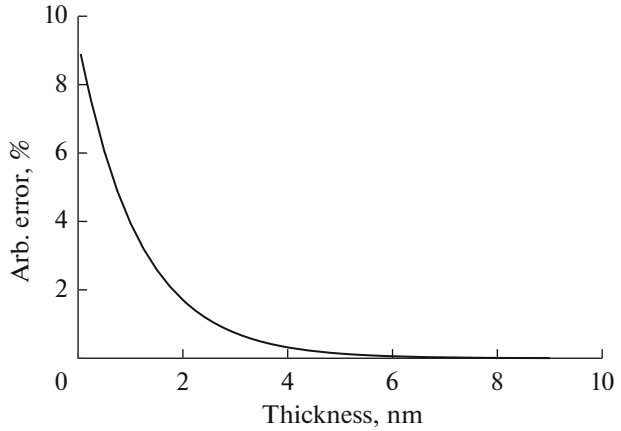

Fig. 9. Error in determining the Ni-layer thickness related to disregarding the processes of elastic photoelectron reflection from the underlying Au layer. Probing is at an angle of 70° to the normal, and the measurement is along the normal to the Ni/Au targets. The Ni-layer thickness is plotted on the abscissa axis.

ACKNOWLEDGMENTS

This work was supported by the Russian Science Foundation (project no. 16-19-10027).

REFERENCES

1. C. S. Fadley, R. J. Baird, W. Siekhaus, T. Novakov, and S. L. Bergstrom, J. Electron Spectrosc. Relat. Phenom. **4**, 93 (1974).
2. C. J. Powell and A. Jablonsky, J. Electron Spectrosc. Relat. Phenom. **178–179**, 331 (2010).
3. S. Hofmann, *Auger and X-Ray Photoelectron Spectroscopy in Material Science* (Springer, Berlin, Heidelberg, 2013).
4. M. Trzhaskovskaya, V. Nefedov, and Y. Yarzhemsky, At. Data Nucl. Data Tables **77**, 97 (2001).
5. M. Trzhaskovskaya, V. Nefedov, and Y. Yarzhemsky, At. Data Nucl. Data Tables **82**, 257 (2002).
6. S. Tanuma, C. J. Powell, and D. R. Penn, Surf. Interface Anal. **37**, 1 (2005).

7. S. Tanuma, C. J. Powell, and D. R. Penn, Surf. Interface Anal. **43**, 689 (2011).
8. K. Stamnes and P. Conklin, J. Quant. Spectrosc. Radiat. Transfer **31**, 273 (1984).
9. K. Stamnes, S. C. Tsay, W. Wiscombe, and K. Jayaweera, Appl. Opt. **27**, 2502 (1988).
10. G. C. Wick, Z. Phys. **121**, 702–718 (1943). doi 10.1007/BF01339167
11. H. van de Hulst, *A New Look at Multiple Scattering, Technical Report* (NASA Institute for Space Studies, New York, 1963).
12. P. C. Waterman, J. Opt. Soc. Am. **71**, 410 (1981). doi doi 10.1364/JOSA.71.000410
13. A. Doicu and T. Trautmann, J. Quant. Spectrosc. Radiat. Transfer **110**, 159 (2009). doi 10.1016/j.jqsrt.2008.09.013
14. D.S. Efremenko, V. Molina Garcia, S. Gimeno Garcia, A.Doicu, J. Quant. Spectrosc.Radiat. Transfer **196**, 17 (2017). doi 10.1016/j.jqsrt.2017.02.015
15. V. P. Afanas'ev, D. S. Efremenko, D. A. Ivanov, P. S. Kaplya, and A. V. Lubenchenko, J. Surf. Invest.: X-ray, Synchrotron Neutron Tech. **8**, 71 (2014). doi 10.1134/S1027451014010030
16. V. P. Afanas'ev and P. S. Kaplya, J. Surf. Invest.: X-ray, Synchrotron Neutron Tech. **9**, 715 (2015).
17. V. P. Afanas'ev, P. S. Kaplya, and E. D. Lisitsyna, J. Surf. Invest.: X-ray, Synchrotron Neutron Tech. **10**, 326–331 (2016). doi 10.1134/S1027451016010043
18. W. S. M. Werner, K. Glantschnig, and C. Ambrosch-Draxl, J. Phys. Chem. Ref. Data **38**, 1013 (2009).
19. V. P. Afanas'ev and P. S. Kaplya, J. Surf. Invest.: X-ray, Synchrotron Neutron Tech. **11**, 1296 (2017). doi 10.1134/S1027451017050226
20. S. Tougaard, J. Electron Spectrosc. Relat. Phenom. **178–179**, 128 (2010).
21. A. Jablonski and J. Zemek, Surf. Interface Anal. **41**, 193 (2009),
22. S. Tanuma, C. J. Powell, and D. R. Penn, Surf. Interface Anal. **35**, 268 (2003).
23. A. Jablonski, F. Salvat, and C. J. Powell, NIST Electron Elastic Scattering Cross, Section Database, Version 3.1 (2003).

Translating by L. Kulman